PASJ: Publ. Astron. Soc. Japan **56**, L45–L48, 2004 December 25

Offsets between Hα and CO Arms of a Spiral Galaxy, NGC 4254: A New Method for Determining the Pattern Speed of Spiral Galaxies

Fumi EGUSA, Yoshiaki SOFUE, and Hiroyuki NAKANISHI
Institute of Astronomy, The University of Tokyo, 2-21-1 Osawa, Mitaka, Tokyo 181-0015
fegusa@ioa.s.u-tokyo.ac.jp, sofue@ioa.s.u-tokyo.ac.jp, hnakanis@ioa.s.u-tokyo.ac.jp

(Received 2004 September 8; accepted 2004 October 8)

Abstract

We examined the offsets between H II regions and molecular clouds belonging to spiral arms of a late-type spiral galaxy, NGC 4254 (M 99). We used a high-resolution ^{12}CO (J = 1–0) image obtained by Nobeyama Millimeter Array (NMA) and an Hα image. We derived angular offsets (θ) in the galactic disk, and found that they show a linear dependence on the angular rotation velocity of the gas ($\Omega_{\rm G}$). This linear relation can be expressed by the equation $\theta = (\Omega_{\rm G} - \Omega_{\rm P}) \cdot t_{\rm H\alpha}$, where $\Omega_{\rm P}$ and $t_{\rm H\alpha}$ are constant. Here, $\Omega_{\rm P}$ corresponds to the pattern speed of the spiral arms and $t_{\rm H\alpha}$ is interpreted as being the timescale between the peak compression of the molecular gas in the spiral arms and the peak of massive star formation. We could thus determine $\Omega_{\rm P}$ and $t_{\rm H\alpha}$ simultaneously by fitting a line to our θ–$\Omega_{\rm G}$ plot, if we assume they are constant. From the plot for NGC 4254, we obtained $t_{\rm H\alpha} = (4.8 \pm 1.2) \times 10^6$ yr and $\Omega_{\rm P} = 26^{+10}_{-6}$ km s^{-1} kpc^{-1}, which are consistent with previous studies. We suggest that this θ–$\Omega_{\rm G}$ plot can be a new tool to determine the pattern speed and the typical timescale needed for star formations.

Key words: galaxies: fundamental parameters — galaxies: individual (M 99, NGC 4254) — galaxies: spiral — ISM: H II region — ISM: molecules

1. Introduction

1.1. Pattern Speed

The pattern speed ($\Omega_{\rm P}$) is defined as the angular rotation velocity of a spiral pattern. According to the spiral density wave theory (Lin, Shu 1964), $\Omega_{\rm P}$ determines the location, and even the existence of resonances, which would greatly affect the morphology and kinematics of a galaxy. The results of numerical simulations also show a large dependence of the spiral structure on $\Omega_{\rm P}$ (Sempere et al. 1995). Despite its importance in the study of galaxies, it cannot be determined directly from observations, since the pattern structure is not a material, but a density wave propagating through the disk.

Several methods have been proposed to date for determining the pattern speed. Tremaine and Weinberg (1984) presented a method using the continuity equation for the surface brightness of galaxies. Canzian (1993) showed that the residual velocity field, obtained by subtracting the axisymmetric component from the observed velocity field, has a difference in pattern between the inside and outside of the corotation. Cepa and Beckman (1990) pointed out that where the arm-to-interarm ratio of the star-formation efficiency has a sharp dip could be thought of as corotation. These methods work well for some galaxies, but there are still inconsistencies or large uncertainties.

1.2. CO and Hα

In this letter, we consider offsets between Hα and CO arms of a spiral galaxy. We suggest that we can use them as a new method for determining the pattern speed and typical timescale for star formation.

Hα emission is a tracer of the H II region, which surrounds newly born massive stars, while CO emission is a tracer of molecular gas. According to the galactic shock-wave theory (Fujimoto 1968; Roberts 1969), most molecular clouds are formed and then condense due to compression, owing to a spiral shock wave, and thus belong to the spiral arm. Since galactic-scale star formations take place in these molecular arms, some molecular gases are used to form stars, and others are dissociated by UV emission from massive stars born in that star formation. In consequence, molecular clouds disappear soon after their formation, and their positions appear to be fixed to the spiral pattern, though individual molecular clouds move at the speed of the gas. Therefore, the position of the spiral pattern and the Hα arm can be measured by using that of a molecular arm and an ensemble of H II regions, respectively. In other words, the offset between the arms of Hα and CO represents the difference between the speeds of the gas and the spiral pattern, as well as the time needed for star formation from molecular clouds.

This offset has been found in many spiral galaxies (e.g., Rand, Kulkarni 1990). We can easily see it in a B-band image as a displacement of an arm's peak and a dust lane, since the light of the B-band is mainly emitted by a young OB star, and the distributions of the dust lane and molecular gas are almost the same. However, this offset has not yet been studied quantitatively, since the resolution of the CO image was too large to examine the detailed structures of the spiral arms.

2. A Method for Determining the Pattern Speed

We assume that the pattern of a spiral is rigid, and that the gas rotates in a circular orbit. Then, we define a timescale, $t_{\rm H\alpha}$, as the *average* time for an Hα arm to develop from a galactic-shock-compressed molecular arm. If the physical processes of star formation are not extremely different in the spiral disk,

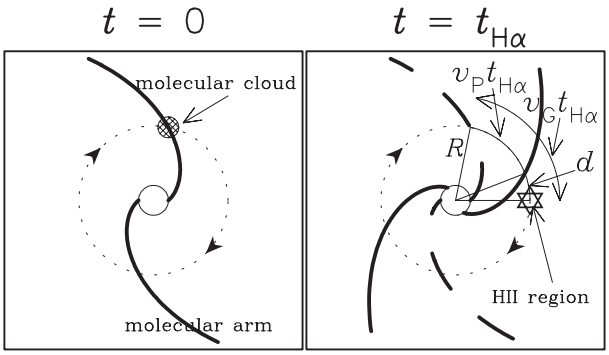

Fig. 1. Basic idea of our method. If we observe a face-on spiral galaxy at $t = 0$ (the left panel), the same galaxy will be observed as the right panel at $t = t_{H\alpha}$. The thick solid lines are molecular arms at time t of each panel. The thick dashed lines in the right panel ($t = t_{H\alpha}$) show the position of the molecular arms in the left panel ($t = 0$). The offset distance between the Hα and CO arms is d, expressed in equation (1).

this timescale can be regarded as being a constant parameter representing a typical value of the entire disk.

Figure 1 illustrates this idea for the inside of the corotation (CR). If we observe a face-on spiral galaxy at $t = 0$ (the left panel), at $t = t_{H\alpha}$ the same galaxy will be observed as the right panel and the offset distance between the arms of Hα and CO, d, can be written as

$$d = \left(\frac{v_G}{\mathrm{km\,s^{-1}}}\right)\left(\frac{t_{H\alpha}}{\mathrm{s}}\right) - \left(\frac{v_P}{\mathrm{km\,s^{-1}}}\right)\left(\frac{t_{H\alpha}}{\mathrm{s}}\right)\ [\mathrm{km}], \qquad (1)$$

where v_G is the velocity of gas, and v_P is the velocity of pattern. We adopt this expression, in which d becomes a positive value, since most molecules exist in a rather central part of the disk, and thus they seem to be in the inside of the CR. If molecular gas is more extended and the outside of the CR should be taken into account, the Hα arm would be seen on the concave side of the CO arm, and d would be negative.

Dividing both sides of equation (1) by radius R [kpc], we obtain

$$\theta = \left[\left(\frac{\Omega_G}{\mathrm{km\,s^{-1}\,kpc^{-1}}}\right) - \left(\frac{\Omega_P}{\mathrm{km\,s^{-1}\,kpc^{-1}}}\right)\right]\left(\frac{t_{H\alpha}}{\mathrm{s}}\right) [\mathrm{km\,kpc^{-1}}], \qquad (2)$$

where $\Omega_G \equiv v_G/R$, $\Omega_P \equiv v_P/R$, and θ is the azimuthal offset. This equation shows the relation between two observables, Ω_G and θ, and we can rewrite it as

$$\theta \simeq 0.58(\Omega_G - \Omega_P)t_{H\alpha}, \qquad (3)$$

where θ is in degree and $t_{H\alpha}$ is in 10^7 yr. If we assume that $t_{H\alpha}$ is constant in a certain range of the radius in a galaxy, θ becomes a linear function of Ω_G, since we assume a rigid pattern, in other words, a constant Ω_P. Therefore, by plotting θ against Ω_G and fitting them with a line, both Ω_P and $t_{H\alpha}$ can be determined at the same time. In addition, the linearity of this plot can verify the validity of the assumptions we made. We discuss this validity in section 4.

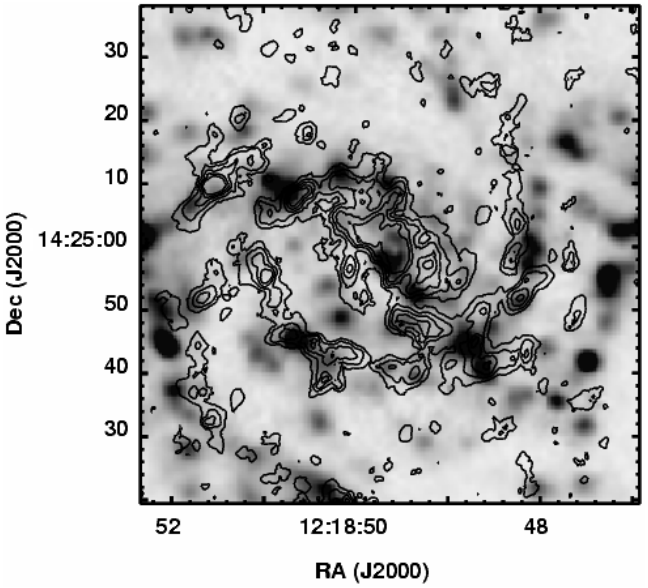

Fig. 2. Projected image of NGC 4254: CO contours on an Hα image.

3. Data

We observed a SAc galaxy, NGC 4254, in the ^{12}CO (J = 1–0) line using the Nobeyama Millimeter Array during a long-term project, "Virgo high resolution CO survey" (Sofue et al. 2003a). The spatial resolution is about 2″, which corresponds to ~ 160 pc at a distance from the Virgo cluster of 16.1 Mpc. This resolution is small enough to trace the spiral arms with a typical width of 1 kpc. For more detailed information about this galaxy and the CO observation, see Sofue et al. (2003c).

Koopmann et al. (2001) presented broadband R and narrow-band Hα images of 63 spiral galaxies in the Virgo cluster. The resolution of the image was 1.″2, comparable to that of our CO data. We determined the coordinates of the Hα image using the stars in our Galaxy seen in the R band image, since these two images had the same field of view. The typical uncertainty of this coordinate fitting is about 1″, smaller than the resolution of the images. We show an overlaid image of CO and Hα in figure 2.

As we can see in this figure, this galaxy is nearly face-on. (We derived an inclination angle of 34° for the central region. See the following paragraph for detail.) It has well-ordered spiral arms [classified as arm class 9 by Elmegreen and Elmegreen (1987)], so that the spiral structure can be easily traced. This is why we selected this galaxy to examine the offsets between the Hα and CO arms.

The position angle (P.A.) and the inclination (i) are also important parameters of a galaxy. We determined them by applying the task 'GAL' of AIPS to the velocity field of CO. This task cuts annuli out from a velocity field, and fits them with a pure circular rotation velocity field in order to derive P.A. and i at each radius. We averaged the derived values at $5'' < R < 16''$, corresponding to $0.4\,\mathrm{kpc} < R < 1.2\,\mathrm{kpc}$, where the values do not change very much, and then obtained P.A. $= 72° \pm 4°$ and $i = 34° \pm 5°$. In table 1, these P.A. and i are listed along with values from other papers. Although only the

Table 1. Position angle and inclination of NGC 4254.

Authority	P.A. [°]	i [°]
Schweizer (1976)	58	29
Iye et al. (1982)	70	42
Phookun et al. (1993)	68	42
This letter (2004)	72	34

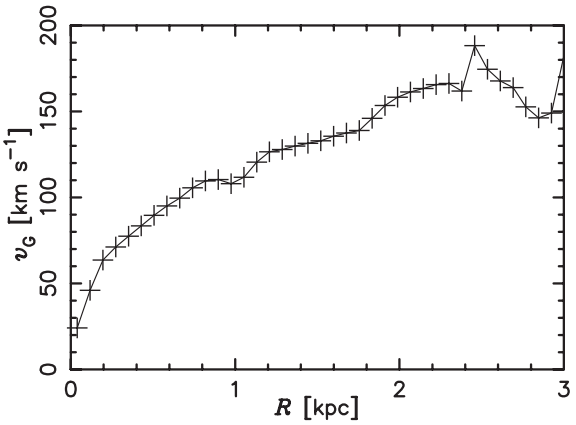

Fig. 3. Rotation curve of NGC 4254, determined by the CO velocity field.

central region was used in this work, the determined values are not so different from these given in previous works, in most of which the whole image of the galaxy was used for the determination.

Using the obtained P.A. and i, we calculated the rotation velocity of gas by using GAL again. The resultant rotation curve (figure 3) is not perfectly the same as that derived by the iteration method (Takamiya, Sofue 2002; Sofue et al. 2003b), since they used different values of P.A. and i.

These P.A. and i were also used to deproject the image into a face-on view and to transform it into a polar-coordinate image, a phase diagram (figure 4). The azimuth is taken to be zero at the NW side of minor axis and to increase clockwise, in the same direction of this galaxy's rotation, assuming the trailing arms. The range between the two horizontal lines in this figure (1 kpc $< R <$ 2.6 kpc) show the region used in a following analysis. The filled boxes and circles are the peaks of the Hα and CO intensities, respectively. See the following section for details.

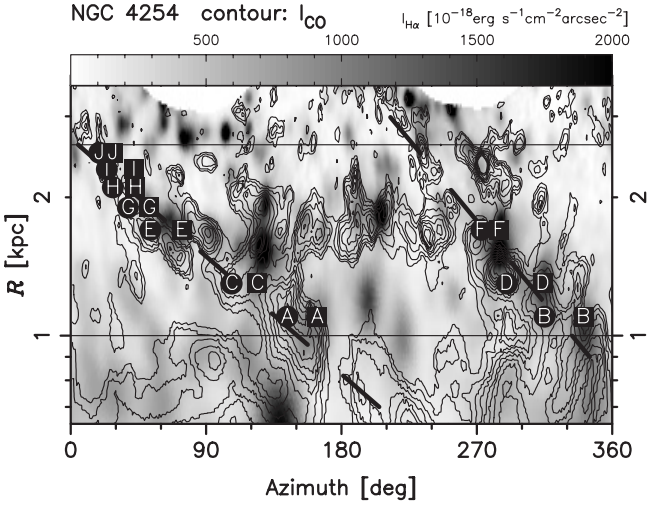

Fig. 4. Phase diagram of NGC 4254: CO contours on Hα image. Thick dashed lines indicate rough positions of two marked spiral arms. Filled circles and boxes are the peaks of CO arm and Hα arm, respectively, which are defined by the analysis described in section 4. Labels, from A to J, are to identify these peaks and offsets presented in figure 5. The region between the two horizontal lines (1 kpc $< R <$ 2.6 kpc) indicates where we used in the analysis.

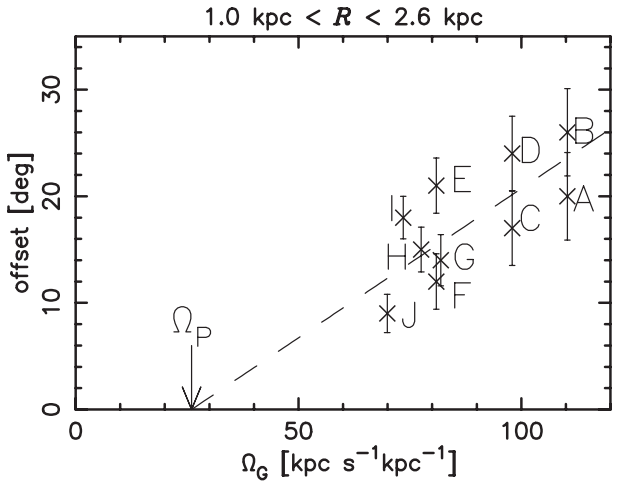

Fig. 5. Plot of the offset angles against the angular rotation velocity. The labels, from A to J, are to identify the offsets, corresponding to the intensity peaks in figure 4. The errorbars were calculated from equation (4) and the dashed line is the fitted line obtained by the χ-square method. The horizontal-axis-intercept and the gradient of this line correspond to Ω_P and $t_{H\alpha}$, respectively.

4. Application and Result

4.1. Deriving Offsets

We divided the phase diagram into strips of 200 pc radial width, averaged the intensity with respect to the radius at each azimuth in each strip, and plotted the averaged intensity against the azimuth. We defined the offset angle, θ, as an azimuthal angular separation of the intensity peaks between the Hα and CO arms. Since the arms of this galaxy are not totally continuous and have some breaks, we could not find corresponding peaks at some radii. In addition, we only used the range of 1 kpc $< R <$ 2.6 kpc, since the spiral feature is not clear in the inner region and the rotation curve has a large dispersion in the outer region (see figure 3). In figure 4, this range is indicated by two horizontal lines. The peaks of the CO and Hα arms are marked by filled circles and boxes, respectively, with the labels from A to J, corresponding to that in figure 5.

The largest factor for the error in θ is the resolution of the CO data, which is about 2″. Thus, this error is written as

$$\Delta\theta \simeq 8.9 \times \left(\frac{R}{\mathrm{kpc}}\right)^{-1} [^\circ]. \quad (4)$$

In addition, the uncertainty of the coordinate fitting of the Hα image and the fact that the determination of offset angles is somewhat subjective would also be possible sources of error in θ. We, however, neglected these errors for simplicity of calculations, so that the error in θ could be larger than the value obtained from equation (4) by a factor of 2, at most.

4.2. Fitting

We plotted the derived offsets against Ω_G, derived from the rotation curve in figure 5. The errorbars in the offset angle are $\Delta\theta$, calculated from equation (4) at each radius. We used the χ-square fitting method and obtained $t_{\mathrm{H}\alpha} = (4.8 \pm 1.2) \times 10^6$ yr and $\Omega_\mathrm{P} = 26^{+10}_{-6}\,\mathrm{km\,s^{-1}\,kpc^{-1}}$. The dashed line in figure 5 is the fitted line, and the gradient and horizontal-axis-intercept of this line corresponds to the resultant value of $t_{\mathrm{H}\alpha}$ and Ω_P, respectively.

Kranz et al. (2001) showed that the corotation radius of NGC 4254 is about 7.5 kpc from numerical simulations, and the corresponding Ω_P is about $20\,\mathrm{km\,s^{-1}\,kpc^{-1}}$. They assumed the distance to the galaxy to be 20 Mpc. If we adjust this result to a distance of 16.1 Mpc, Ω_P should be about $25\,\mathrm{km\,s^{-1}\,kpc^{-1}}$. The typical timescale of star formation has been suggested to be about 10^7 yr from a calculation of the Jeans time in molecular clouds. Our results are in good agreement with these previous studies.

4.3. Discussion

In our method, we assumed a pure circular rotation and a constant time delay for star formation from molecular clouds, and did not make any correction for extinction in the Hα data. We however know that deviations from these assumptions are not critically large. The streaming motion and the velocity dispersion would generate some non-circular motion, but in a spiral disk these are usually about $10\,\mathrm{km\,s^{-1}}$ (Adler, Westpfahl 1996; Combes, Becquaert 1997), which is very small compared to the circular rotation velocity of $\sim 100\,\mathrm{km\,s^{-1}}$. The validity of the latter assumption, constant $t_{\mathrm{H}\alpha}$, can be checked by the linearity of θ–Ω_G plot (figure 5). Since this plot is well fitted with a line, the dependence of $t_{\mathrm{H}\alpha}$ on the environment should be small, and included in the error of the derived value.

The extinction of Hα is surely significant to the luminosity, and this might lead us to overestimate the offset values, since the amount of extinction becomes larger as the H II regions become closer to the molecular arms, and an Hα arm thus seems to shift to the downstream side from where it really is. González and Graham (1996) showed azimuthal brightness profiles of NGC 4254 in K_s-, g-, and r_s-band image at $R = 75''$ (figure 20 in their paper). Though the shape of the profile is different from one to another, the positions of the peak brightness are very consistent among them. Hence, we can assume that the extinction would hardly change the position of the Hα arms, and neglect the effect of extinction on the offset values.

5. Conclusion

We examined the offset between the arms of Hα and CO of the SAc galaxy NGC 4254, derived ten offset values and found a linear relation between the offset angle and the angular rotation velocity. This linearity implies that a rigid spiral pattern exists, and that the physical processes of star formation can be regarded as not to extremely change in the disk. We emphasize that this is the first work to show this relationship.

With this relation, we derived the pattern speed, $\Omega_\mathrm{P} = 26^{+10}_{-6}\,\mathrm{km\,s^{-1}\,kpc^{-1}}$, and the time delay for star formation, $t_{\mathrm{H}\alpha} = (4.8 \pm 1.2) \times 10^6$ yr. We again emphasize that we can derive both Ω_P and $t_{\mathrm{H}\alpha}$ simultaneously. Since the obtained values are consistent with previous studies, the way of our analysis can be a new method for the determination of the pattern speed and the typical timescale needed for star formations. Thus, this method can investigate not only the kinematics, but also the star-formation mechanisms quantitatively. Moreover, this method can be applied to many spiral galaxies, since the offsets between the Hα and CO arms have been found in many spirals.

We are very grateful to Rebecca A. Koopmann, Jeffrey D. P. Kenney, and Judith Young for kindly providing us with their R and Hα image of NGC 4254. H.N. is financially supported by a Research Fellowship from the Japan Society for the Promotion of Science for Young Scientists.

References

Adler, D. S., & Westpfahl, D. J. 1996, AJ, 111, 735
Canzian, B. 1993, ApJ, 414, 487
Cepa, J., & Beckman, J. E. 1990, ApJ, 349, 497
Combes, F., & Becquaert, J.-F. 1997, A&A, 326, 554
Elmegreen, D. M., & Elmegreen, B. G. 1987, ApJ, 314, 3
Fujimoto, M. 1968, in Non-stable Phenomena in Galaxies, IAU Symp., 29, 453
González, R. A., & Graham, J. R. 1996, ApJ, 460, 651
Iye, M., Okamura, S., Hamabe, M., & Watanabe, M. 1982, ApJ, 256, 103
Koopmann, R. A., Kenney, J. D. P., & Young, J. 2001, ApJS, 135, 125
Kranz, T., Slyz, A., & Rix, H.-W. 2001, ApJ, 562, 164
Lin, C. C., & Shu, F. H. 1964, ApJ, 140, 646
Phookun, B., Vogel, S. N., & Mundy, L. G. 1993, ApJ, 418, 113
Rand, R. J., & Kulkarni, S. R. 1990, ApJ, 349, L43
Roberts, W. W. 1969, ApJ, 158, 123
Schweizer, F. 1976, ApJS, 31, 313
Sempere, M. J., García-Burillo, S., Combes, F., & Knapen, J. H. 1995, A&A, 296, 45
Sofue, Y., Koda, J., Nakanishi, H., & Hidaka, M. 2003c, PASJ, 55, 75
Sofue, Y., Koda, J., Nakanishi, H., & Onodera, S. 2003b, PASJ, 55, 59
Sofue, Y., Koda, J., Nakanishi, H., Onodera, S., Kohno, K., Tomita, A., & Okumura, S. K. 2003a, PASJ, 55, 17
Takamiya, T., & Sofue, Y. 2002, ApJ, 576, L15
Tremaine, S., & Weinberg, M. D. 1984, ApJ, 282, L5